Research Article | Vol. 26, No. 17 | 20 Aug 2018 | OPTICS EXPRESS 21969
Optics EXPRESS

Realization of simultaneously parity-time-symmetric and parity-time-antisymmetric susceptibilities along the longitudinal direction in atomic systems with all optical controls

YOU-LIN CHUANG,[1,*] ZIAUDDIN,[2] AND RAY-KUANG LEE[1,3]

[1] *Physics Division, National Center for Theoretical Sciences, Hsinchu, Taiwan*
[2] *Department of Physics, COMSATS University, Islamabad, Pakistan*
[3] *Institute of Photonics Technologies, National Tsing Hua University, Hsinchu, Taiwan*
[*] *yloptics@cts.nthu.edu.tw*

Abstract: We propose an all-optical-control scheme to simultaneously realize parity-time ($\mathscr{P}\mathscr{T}$)-symmetric and $\mathscr{P}\mathscr{T}$-antisymmetric susceptibilities along the propagation direction of light by applying an external magnetic field. Through the light-atom interaction within a double-Λ configuration, the resulting position-dependent susceptibilities for the interacting fields can be manipulated through the relative phase between them. In particular, for the probe field, one can switch its refractive index from the $\mathscr{P}\mathscr{T}$-symmetry to $\mathscr{P}\mathscr{T}$-antisymmetry by just varying the phase. Based on the quantum interference among transition channels in a closed loop, analytical formulas are also derived to illustrate the conditions for $\mathscr{P}\mathscr{T}$-symmetry and $\mathscr{P}\mathscr{T}$-antisymmetry.

1. Introduction

Even though parity-time ($\mathscr{P}\mathscr{T}$) symmetry was initially introduced to generalize quantum mechanics with Hermitian Hamiltonians to non-Hermitian ones [1], quantum entanglement gives negative results for the no-signalling principle when applying the local $\mathscr{P}\mathscr{T}$-symmetric operation on one of the entangled particles [2]. Nevertheless, $\mathscr{P}\mathscr{T}$-symmetry could still be used as an interesting model for open systems in the classical limit [3].

In classical optics, with the correspondence between paraxial wave equation and Schrodinger equation, one can realize optical $\mathscr{P}\mathscr{T}$-symmetric systems by asking the refractive index in the medium to satisfy some specific symmetries. For non-magnetic materials, $\mathscr{P}\mathscr{T}$-symmetric condition is said to be satisfied when the optical susceptibility χ has the form: $\chi(\eta) = \chi^*(-\eta)$. Here, the spatial coordinate η can be a transverse or longitudinal one, with respect to the propagation direction. One can see that such a sufficient condition for $\mathscr{P}\mathscr{T}$-symmetry requires an even function in the real part of susceptibility, along with an odd function in the imaginary part. The latter one corresponds to a perfect balance between gain and loss [4, 5]. Moreover, in stead of embedding gain or loss mechanics to implement $\mathscr{P}\mathscr{T}$-symmetry [6], one can also have $\mathscr{P}\mathscr{T}$-antisymmetry by asking the susceptibility in the form, $\chi(\eta) = -\chi^*(-\eta)$ [7, 8].

With the addition degree of freedom from a non-conservative Hamiltonian, as well as the existence of exceptional points to induce phase transition due to the broken $\mathscr{P}\mathscr{T}$-symmetry [9], optical $\mathscr{P}\mathscr{T}$-symmetric devices are studied theoretically and experimentally for directional couplers [10, 11], optical lattices [12–14], soliton dynamics [15], wave localization [16, 17], Bloch oscillations [18], and light diffraction [19]. In addition to play with the optical refractive index directly, $\mathscr{P}\mathscr{T}$-symmetric conditions can also be realized in different physical systems, such as whispering-gallery microcavities [20], moving media [21], RLC circuits [22], and optomechanically-induced transparency systems [23].

#330585 https://doi.org/10.1364/OE.26.021969
Journal © 2018 Received 30 Apr 2018; revised 26 Jul 2018; accepted 27 Jul 2018; published 9 Aug 2018

Optics EXPRESS

In terms of optical refractive index, it is well-known that one can manipulate optical properties of a probe field through the light-atom interaction [24]. As a consequence, a variety of configurations for atom-photon interactions have been proposed and demonstrated to realize $\mathscr{P}\mathscr{T}$-symmetric systems in different experimental settings [25–29]. Even though there already exist many schemes to have $\mathscr{P}\mathscr{T}$-symmetry and $\mathscr{P}\mathscr{T}$-antisymmetry, a single scheme to simultaneously realize both of them is still missing. Here, we propose a scheme to realize $\mathscr{P}\mathscr{T}$-symmetric and $\mathscr{P}\mathscr{T}$-antisymmetric susceptibilities for probe and signal fields passing through an atomic system in a double-Λ configuration [30]. By using an external magnetic field with its magnitude linearly increasing along the propagation direction, the position-dependent Zeeman effect can map the intrinsic symmetry or antisymmetry in the optical susceptibilities with respect to the frequency detuning into the direction of propagation. Then, $\mathscr{P}\mathscr{T}$-symmetry and $\mathscr{P}\mathscr{T}$-antisymmetry in the susceptibilities can be controlled by all optical approaches. Simultaneous realizations of $\mathscr{P}\mathscr{T}$-symmetry-antisymmetry or $\mathscr{P}\mathscr{T}$-antisymmetry-antisymmetry in the probe-signal fields will be illustrated by varying the relative phase between these two fields. The potential applications of $\mathscr{P}\mathscr{T}$-symmetry and $\mathscr{P}\mathscr{T}$-antisymmetry in the longitudinal direction include coherent perfect absorbers [31–34], unidirectional invisibility [35–38], and unidirectional light reflection [39]. Further, the $\mathscr{P}\mathscr{T}$-symmetry in the longitudinal direction has the flexibility for real time control, all optical tuning, and re-configuration.

This paper is organized as following. In Sec. 2, we will give the light-atom interaction Hamiltonian for a double-Λ configuration, with the corresponding optical susceptibilities for probe and signal fields, respectively. Then, in Sec. 3, illustrations on the simultaneous realization of $\mathscr{P}\mathscr{T}$-symmetry and $\mathscr{P}\mathscr{T}$-antisymmetry in the susceptibilities of probe and signal fields are shown along the propagation distance. The underline physical picture and discussions will be given with the analytical formula in Sec. 4. Finally, we summary this work in Sec. 5.

2. Field susceptibilities in a double-Λ atomic system

We consider a photon-atom interaction system with allowable transitions in a four-level double-Λ configuration, as shown in Fig. 1. Here, we have four interacting fields, including two weak (denoted as probe and signal) fields and two strong (denoted as coupling and driving) fields. The corresponding transitions are characterized by its Rabi frequencies, denoted as Ω_p, Ω_s, Ω_c, and Ω_d, respectively. Then, the one-photon detunings of these four fields are defined as $\Delta_p = \omega_p - \omega_{31}$, $\Delta_s = \omega_s - \omega_{41}$, $\Delta_c = \omega_c - \omega_{32}$, and $\Delta_d = \omega_d - \omega_{42}$, where the notations ω_μ ($\mu \in p,s,c,d$) and $\omega_{\mu\nu} \equiv \left(E_\mu - E_\nu\right)/\hbar$ represent the field frequency and the corresponding energy difference between energy states $|\mu\rangle$ and $|\nu\rangle$, respectively.

With the rotating wave approximation, one can write down the interaction Hamiltonian for this four-level atomic system in a double-Λ configuration:

$$\begin{aligned}\hat{H} = &-\hbar\left[\Delta_p|3\rangle\langle 3| + \left(\Delta_p - \Delta_c\right)|2\rangle\langle 2| + \Delta_s|4\rangle\langle 4|\right] \\ &-\frac{\hbar}{2}\left(\Omega_p|3\rangle\langle 1| + \Omega_c|3\rangle\langle 2| + \Omega_s|4\rangle\langle 1| + \Omega_d|4\rangle\langle 2| + H.C.\right).\end{aligned} \tag{1}$$

Here, we have asked the detunings to satisfy the condition: $\Delta_p + \Delta_d - \Delta_s - \Delta_c = 0$, corresponding to a zero net detuning. Moreover, as the intensities of probe and signal fields are much weaker than those of coupling and driving fields, i.e., $\Omega_p, \Omega_s \ll \Omega_c, \Omega_d$, one can safely derive the equations of motion for density matrix elements in the lowest order, which have the form:

$$\frac{\partial}{\partial t}\rho_{21} = -\tilde{\gamma}_{21}\rho_{21} + \frac{i}{2}\Omega_c^*\rho_{31} + \frac{i}{2}\Omega_d^*\rho_{41}, \tag{2}$$

$$\frac{\partial}{\partial t}\rho_{31} = -\tilde{\gamma}_{31}\rho_{31} + \frac{i}{2}\Omega_c\rho_{21} + \frac{i}{2}\Omega_p, \tag{3}$$

$$\frac{\partial}{\partial t}\rho_{41} = -\tilde{\gamma}_{41}\rho_{41} + \frac{i}{2}\Omega_d\rho_{21} + \frac{i}{2}\Omega_s. \tag{4}$$

Optics EXPRESS

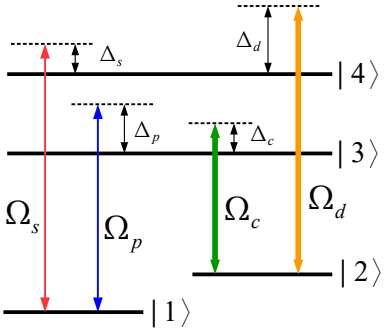

Fig. 1. Our four-level atomic system in a double-Λ configuration. Here, the four fields are denoted as Ω_s, Ω_p, Ω_c, and Ω_d, with the corresponding Rabi frequencies for signal, probe, coupling, and driving fields, respectively. The one-photon detunings of these fields are characterized by Δ_s, Δ_p, Δ_c, and Δ_d, respectively.

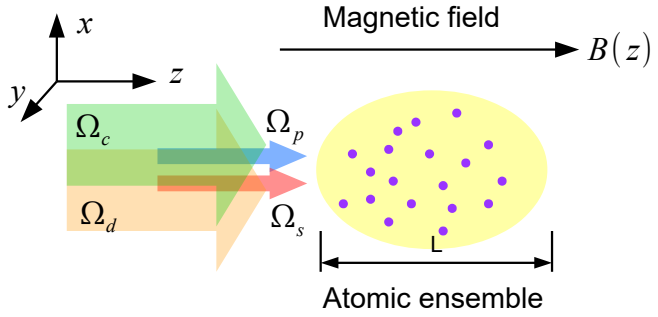

Fig. 2. Setup of our photon-light interaction scheme, where four fields propagate along the z-direction and the atomic ensemble having photon-atom interaction in a double-Λ configuration, as shown in Fig. 1. With a magnetic field B(z), which has its magnitude linearly increasing along the propagation z-direction, the resulting susceptibilities for probe and signal fields can support a $\mathscr{P}\mathscr{T}$-symmetry or $\mathscr{P}\mathscr{T}$-antisymmetry in the longitudinal z-direction.

Here, decays in the upper atomic levels ($|e\rangle$, $e = 2,3,4$) to the ground state ($|1\rangle$) are introduced phenomenologically through $\tilde{\gamma}_{21} \equiv \gamma_{21} - i\left(\Delta_p - \Delta_c\right)$, $\tilde{\gamma}_{31} \equiv \gamma_{31} - i\Delta_p$, and $\tilde{\gamma}_{41} \equiv \gamma_{41} - i\Delta_s$.

Macroscopically, the susceptibility for probe field can be found by collecting the atomic matrix component ρ_{31}, i.e., $\chi_p = \left(n\wp_{31}^2/\varepsilon_0\hbar\Omega_p\right)\rho_{31}$ with the number density of atomic medium, $n = NV$, and the atomic dipole transition from $|1\rangle$ to $|3\rangle$, $\wp_{31}$. For steady states, one can ignore the time derivative terms and obtain the susceptibility of probe field by solving Eqs. (2)-(4), i.e.,

$$\chi_p = \chi_{p0}\left[\frac{i\left(4\tilde{\gamma}_{21}\tilde{\gamma}_{41}\Omega_p + |\Omega_d|^2\Omega_p - \Omega_c\Omega_d^*\Omega_s\right)}{4\tilde{\gamma}_{21}\tilde{\gamma}_{31}\tilde{\gamma}_{41} + \tilde{\gamma}_{41}|\Omega_c|^2 + \tilde{\gamma}_{31}|\Omega_d|^2}\right], \tag{5}$$

where we have defined $\chi_{p0} \equiv n\wp_{31}^2/2\varepsilon_0\hbar\Omega_p = \left(\alpha/8\right)\left(\lambda_p/L\right)\left(\Gamma/\Omega_p\right)$, with the optical density of atomic ensemble denoted by $\alpha = n\sigma L$, the wavelength of probe field λ_p, the length L, the absorption cross section of probe field $\sigma = 3\lambda_p^2/2\pi^2$, and the excited state spontaneous decay rate Γ (associated with $\gamma_{31} = \gamma_{41} = 1.25\Gamma$). It is noted that in general the Rabi frequency of each field is a complex number. As shown in Fig. 1, due to such a closed-loop configuration for

Optics EXPRESS

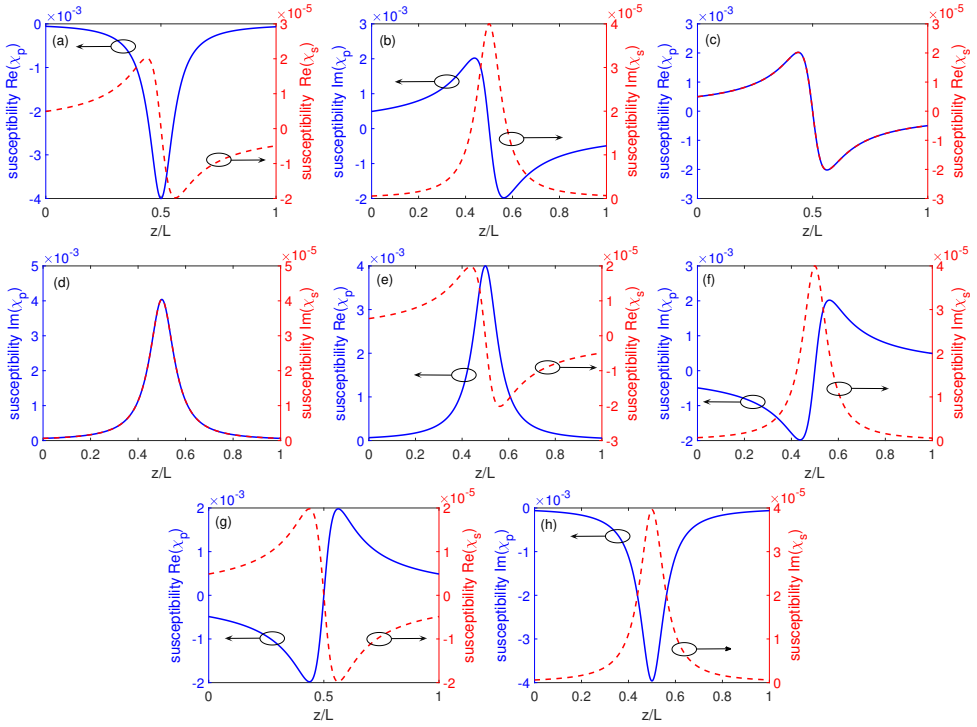

Fig. 3. Real (Left-column) and imaginary (Right-column) parts of the susceptibilities for probe and signal fields, depicted in blue- and red-curves, respectively. The relative phase difference ϕ_r is: (a-b) $\pi/2$, (c-d) π, (e-f) $3\pi/2$, and (g-h) 2π. One can see that χ_p satisfies the $\mathscr{P}\mathscr{T}$-symmetric condition when $\phi_r = \pi/2, 3\pi/2$; and satisfies the $\mathscr{P}\mathscr{T}$-antisymmetric condition when $\phi_r = \pi, 2\pi$. However, χ_s only gives the $\mathscr{P}\mathscr{T}$-antisymmetric condition. Here, the parameters used are $|\Omega_c| = |\Omega_d| = 20\Gamma$, $\Omega_p = 0.01\Gamma$, and $\Omega_s = 1\Gamma$, respectively.

the interaction channels, the relative phase in the form: $\phi_r = \phi_p + \phi_d - \phi_s - \phi_c$, plays a crucial parameter in our system [30].

For the signal field, we can apply the same analysis to have its susceptibility by calculating the density element ρ_{41}. The corresponding susceptibility for signal field can be found as $\chi_s = \left(n\wp_{41}^2/\varepsilon_0\hbar\Omega_s\right)\rho_{41}$, or explicitly in the form:

$$\chi_s = \chi_{s0}\left[\frac{i\left(4\tilde{\gamma}_{21}\tilde{\gamma}_{31}\Omega_s + |\Omega_c|^2\Omega_s - \Omega_d\Omega_c^*\Omega_p\right)}{4\tilde{\gamma}_{21}\tilde{\gamma}_{31}\tilde{\gamma}_{41} + \tilde{\gamma}_{41}|\Omega_c|^2 + \tilde{\gamma}_{31}|\Omega_d|^2}\right]. \tag{6}$$

Here, we have defined $\chi_{s0} = \left(\alpha/8\right)\left(\lambda_s/L\right)\left(\Gamma/\Omega_s\right)$, with the wavelength of signal field λ_s.

3. $\mathscr{P}\mathscr{T}$-symmetry and $\mathscr{P}\mathscr{T}$-antisymmetry in the longitudinal direction

With Eqs. (5)-(6), one can see that, in terms of the frequency detuning of signal field, Δ_s, the corresponding susceptibilities for probe and signal fields are manifested with respect to frequency detuning, but not to spatial coordinate. As a simple way to realize optical $\mathscr{P}\mathscr{T}$-symmetric condition, we propose to apply a magnetic field $B\left(z\right)$ along the propagation direction, z, see Fig. 2. If this magnetic field has a linearly increasing function along the z-direction, the induced Zeeman effect will also be position dependent. Then, as the Zeeman effect splits the energy level,

Optics EXPRESS

we can map the detuning information Δ_s to the longitudinal position, i.e.,

$$\Delta_s(z) = \Delta_s(0) - g_L m_j \mu_B B(z)/\hbar. \tag{7}$$

Here, $\mu_B = e\hbar/2m_e = 9.27 \times 10^{-24}$ (in the unit of Joule/Tesla) is Bohr magneton, and $g_L = 1 + \left[J(J+1) + S(S+1) - L(L+1)\right]/2J(J+1)$ is the Landé g-factor, with S, L, and $J = L+S$ denoting the spin, orbital, and total angular momentums, respectively. Moreover, we have assumed that $B(z=0) = 0$ and $B(z>0) > 0$.

Now, as the detuning Δ_s becomes a linear function along the z-direction, depending on the sign of the quantum number m_j, the corresponding $\Delta_s(0)$ can be positive or negative. By adjusting $B(z)$ and $\Delta_s(0)$, we can implement the symmetry condition of $\Delta_s(L) = -\Delta_s(0)$, with magnetic field in the form:

$$B(z) = \left[\frac{2\hbar\Delta_s(0)}{g_L m_j \mu_B L}\right] z. \tag{8}$$

By taking Rubidium atoms ^{87}Rb as our atomic ensemble, from Eq. (8), one can estimate the gradient of a magnetic field along z-direction as 4.27 (Tesla/m), for $|\Delta_s(0)| = 10\Gamma$, $\Gamma = 2\pi \times 6$ MHz, $g_L = 4/3$, $m_j = 3/2$, and $L \simeq 1$ mm.

Based on this scheme, we can transfer the optical susceptibility from the (detuning) spectrum to a position-dependent distribution. In particular, as shown in Fig. 3, we reveal the susceptibilities of probe and signal fields, i.e., $\chi_p(z)$ and $\chi_s(z)$, in Blue- and Red-curves, respectively, for different relative phases $\phi_r = \pi/2$, π, $3\pi/2$, and 2π.

For probe field, $\chi_p(z)$ in Blue-curves, as one can see, when the relative phase is $\phi_r = (2n+1)\pi/2$, $n \in$ integers, as shown in Figs. 3(a)-3(b) and 3(e)-3(f), the real part of probe susceptibility is an even function; while the imaginary part is an odd function with respect to the center of length. This is the optical $\mathscr{P}\mathscr{T}$-symmetric condition. Moreover, one can see from the real part of susceptibility in Figs. 3(a) and 3(c), we have a negative refractive index for the probe field when $\phi_r = \pi/2$, along with a dip in the central position; while a positive refractive index happens when $\phi_r = 3\pi/2$, along with a peak in the central position.

Nevertheless, when the relative phase is $\phi_r = n\pi$, with $n \in$ integers, as shown in Figs. 3(c)-3(d) and 3(g)-3(h), the real and imaginary parts of χ_p become odd and even functions, respectively. Now, we have the $\mathscr{P}\mathscr{T}$-antisymmetric susceptibility. Moreover, the imaginary part of susceptibility shows that we have a gain peak for $\phi_r = \pi$, but a absorption dip for $\phi_r = 2\pi$. Most importantly, only a change in the relative phase can give us such an all-optical-control to switch from a $\mathscr{P}\mathscr{T}$-symmetry to $\mathscr{P}\mathscr{T}$-antisymmetry or vice versa.

In addition to the probe field, the susceptibility for signal field is also depicted in Fig. 3, but in Red-color. Nevertheless, no matter what the relative phase is, we always have an odd function in the real part of susceptibility for signal field, and an even function in its imaginary part of susceptibility. Here, for signal field, we have the $\mathscr{P}\mathscr{T}$-antisymmetric susceptibility. Moreover, the imaginary part of susceptibility gives a gain peak at the central position. Simultaneously, when $\phi_r = (2n+1)\pi/2$, $n \in$ integers, we can realize $\mathscr{P}\mathscr{T}$-symmetric and $\mathscr{P}\mathscr{T}$-antisymmetric conditions in the susceptibilities of probe and signal fields, respectively. When $\phi = n\pi$, both the susceptibilities of probe and signal fields satisfy the $\mathscr{P}\mathscr{T}$-antisymmetric condition at the same time.

To check the symmetry on the probe susceptibility, we calculate the deviation in the susceptibility by calculating $\left[\xi(z) - \xi(L-z)\right]/\Theta_-$ for an even function and $\left[\xi(z) + \xi(L-z)\right]/\Theta_+$ for an odd function, respectively. Here, ξ can be the real or imaginary part of the susceptibility in the probe or signal field, i.e., $\mathrm{Re}(\chi_p)$, $\mathrm{Im}(\chi_p)$, $\mathrm{Re}(\chi_s)$, or $\mathrm{Im}(\chi_s)$. A normalized factor $\Theta_\pm$ is also introduced, which is defined by the maximal value of $|\xi|$. As an illustration, we fix $\Omega_p = 0.01$ in Fig. 4 for the condition of a small probe intensity. One can see that only a negligible

Optics EXPRESS

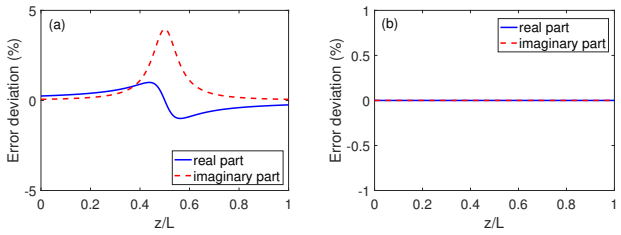

Fig. 4. The deviation of symmetry on the probe susceptibility. For an even function, we calculate $\xi(z)-\xi(L-z)/\Theta_-$; while for an odd function, we calculate $[\xi(z)+\xi(L-z)]/\Theta_+$. Here, ξ can be the real (in blue-color) or imaginary (in red-color) part of the susceptibility in the probe field, and $\Theta_\pm$ is the normalized factor. All the parameters used are the same as those shown in Fig. 3, but the relative phases are choose for (a): $\phi_r = (2n)\times\pi/2$; and (b): $\phi_r = (2n+1)\times\pi/2$.

deviation, i.e., less than 5%, is found in Fig. 4(a) for the relative phase $\phi_r = (2n)\times\pi/2$ and in Fig. 4(b) for the relative phase $\phi_r = (2n+1)\times\pi/2$. These results reveal that the symmetry in our probe susceptibility is almost perfect along the longitudinal direction.

4. Discussions

In order to illustrate the physical picture behind the results of these $\mathscr{PT}$-symmetry and $\mathscr{PT}$-antisymmetry, we can further simplify the susceptibility for probe and signal fields given in Eqs. (5)-(6). First of all, let us consider the condition with the relative phase $\phi_r = \pi/2$ and $|\Omega_c| = |\Omega_d| \gg \Omega_p, \Omega_s$. Then, the corresponding susceptibility of probe field can be approximated as:

$$\mathrm{Re}\chi_p \simeq -\chi_{p0}\left(\frac{\Delta_s\Omega_p + 2\gamma_{31}\Omega_s}{\Delta_s^2+4\gamma_{31}^2}\right), \tag{9}$$

$$\mathrm{Im}\chi_p \simeq \chi_{p0}\left(\frac{2\gamma_{31}\Omega_p - \Delta_s\Omega_s}{\Delta_s^2+4\gamma_{31}^2}\right). \tag{10}$$

From Eqs. (9)-(10), one can see that the real part of probe susceptibility is almost an even function with respect to the frequency detuning Δ_s when $\Omega_s/\Omega_p \gg |\Delta_s|/2\gamma_{31}$. At the same time, the imaginary part of χ_p becomes an odd function. Then, the linear transformation between the detuning Δ_s and propagation distance z maps these even/odd functions into the longitudinal position.

Instead, when the relative phase is set as $\phi_r = 3\pi 2$, the corresponding probe susceptibility χ_p becomes

$$\mathrm{Re}\chi_p \simeq -\chi_{p0}\left(\frac{\Delta_s\Omega_p - 2\gamma_{31}\Omega_s}{\Delta_s^2+4\gamma_{31}^2}\right), \tag{11}$$

$$\mathrm{Im}\chi_p \simeq \chi_{p0}\left(\frac{2\gamma_{31}\Omega_p + \Delta_s\Omega_s}{\Delta_s^2+4\gamma_{31}^2}\right). \tag{12}$$

By comparing Eqs. (9)-(10) and Eqs. (11)-(12), the change of the sign in front of $2\gamma_{31}$ of the numerator gives us an odd function for the real part of probe susceptibility; along with an even function for the imaginary part. According to the discussions above, now we have the $\mathscr{PT}$-symmetric condition.

Optics EXPRESS

Next, when the relative phase is $\phi_r = \pi$ or $\phi_r = 2\pi$, the probe susceptibility can be approximated as:

$$\mathrm{Re}\chi_p \simeq -\chi_{p0}\left(\frac{\Delta_s\left(\Omega_p \pm \Omega_s\right)}{\Delta_s^2 + 4\gamma_{31}^2}\right), \tag{13}$$

$$\mathrm{Im}\chi_p \simeq \chi_{p0}\left(\frac{2\gamma_{31}\left(\Omega_p \pm \Omega_s\right)}{\Delta_s^2 + 4\gamma_{31}^2}\right). \tag{14}$$

Here, the + sign applies for $\phi_r = \pi$, while the $-$ sign applies for $\phi_r = 2\pi$, respectively. As one can see, we have an odd function for real part of probe susceptibility, and an even function for the imaginary part, resulting in the $\mathscr{P}\mathscr{T}$-antisymmetric condition.

As for the signal field, when the relative phase is $\phi_r = \pi/2 \;\; n \in$ integers, Eq. (6) can be approximated as:

$$\mathrm{Re}\chi_s \simeq \chi_{s0}\left(\frac{-\Delta_s\Omega_s \pm 2\gamma_{31}\Omega_p}{\Delta_s^2 + 4\gamma_{31}^2}\right), \tag{15}$$

$$\mathrm{Im}\chi_s \simeq \chi_{s0}\left(\frac{2\gamma_{31}\Omega_s \pm \Delta_s\Omega_p}{\Delta_s^2 + 4\gamma_{31}^2}\right). \tag{16}$$

Here, the sign, + or $-$, applies for even or odd number of n, respectively. Similarly, the signal susceptibilities for the relative phases $\phi_r = \left(2n+1\right) \times \pi, \;\; n \in$ integers and $\phi_r = 2n \times \pi, \;\; n \in$ integers have the forms:

$$\mathrm{Re}\chi_s \simeq -\chi_{s0}\left(\frac{\Delta_s\left(\Omega_s \pm \Omega_p\right)}{\Delta_s^2 + 4\gamma_{31}^2}\right), \tag{17}$$

$$\mathrm{Im}\chi_s \simeq \chi_{s0}\left(\frac{2\gamma_{31}\left(\Omega_s \pm \Omega_p\right)}{\Delta_s^2 + 4\gamma_{31}^2}\right). \tag{18}$$

Again, the sign, + or $-$, applies for even or odd number of n, respectively. Nevertheless, with the comparison to the probe susceptibility, when $\Omega_s/\Omega_p \gg 2\gamma_{31}/|\Delta_s|$, the real part of signal susceptibility is always an odd function, while the imaginary is an even one. It means that the $\mathscr{P}\mathscr{T}$-antisymmetric condition for signal field is fulfilled.

Before the conclusion, let us remark the roles played by the probe and signal fields. In our 4-level double-Λ configuration, the role of Ω_p and Ω_s can be exchanged. Nevertheless, such an even or odd function in the susceptibility comes from the detuning of signal field, Δ_s. That is, if we perform the detuning of probe field, Δ_p, $\mathscr{P}\mathscr{T}$-symmetry can be manifested in the signal field. Moreover, to simultaneously realize $\mathscr{P}\mathscr{T}$-symmetry and $\mathscr{P}\mathscr{T}$-antisymmetry for probe and signal fields, their Rabi frequencies are either $\Omega_p \ll \Omega_s$ or $\Omega_p \gg \Omega_s$. Nevertheless, by only manipulating the relative phase, ϕ_r, one can also change the energy flow between probe and signal fields.

To illustrate the propagation effect on the optical susceptibilities under $\mathscr{P}\mathscr{T}$-symmetric and $\mathscr{P}\mathscr{T}$-antisymmetric conditions, we apply the Maxwell-Schrodinger equations for probe Ω_p and signal Ω_s, i.e.,

$$\frac{\partial\Omega_p}{\partial z} = i\frac{\gamma_{31}\alpha}{2}\rho_{31}, \tag{19}$$

$$\frac{\partial\Omega_s}{\partial z} = i\frac{\gamma_{41}\alpha}{2}\rho_{41}. \tag{20}$$

By solving Eqs. (2)-(4) as well as Eqs. (19)-(20) numerically and taking the spatial dependent detuning given in Eq. (7), we can obtain the field propagation behaviors.

Optics EXPRESS

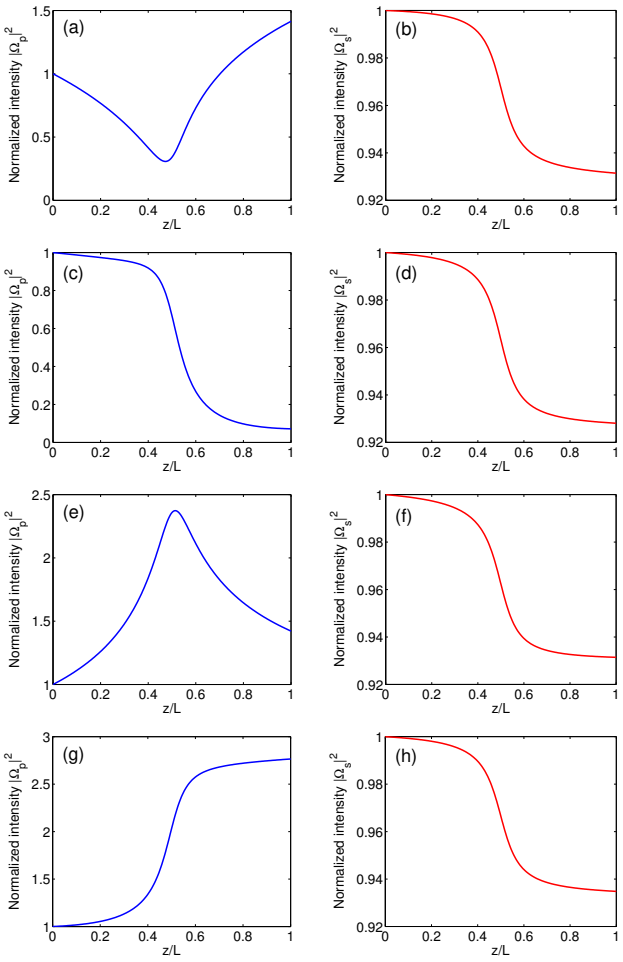

Fig. 5. Probe and signal field intensity verse the propagation distance with different phases: (a,b) $\phi_r = \pi/2$, (c,d) $\phi_r = 2 \times \pi/2$, (e,f) $\phi_r = 3 \times \pi/2$, and (g,h) $\phi_r = 4 \times \pi/2$

In Fig. 5, we reveal the relationships between probe and signal field intensities and propagation distances under different phases ϕ_r. For the probe field with the $\mathscr{P}\mathscr{T}$-symmetry, as shown in Fig. 5(a), it suffers loss in the first half part of medium, and then gets gain in the rest part. It can be understood by Fig. 3(b), in which the imaginary part of probe field susceptibility is positive (loss) from $0 < z < L/2$, and negative (gain) when $L/2 < z < L$. Similarly, when $\phi_r = 3\pi/2$, Fig. 5(e) shows that the probe field gets gain first and loss afterward. On the other hand, the signal field has $\mathscr{P}\mathscr{T}$-antisymmetry condition, which means that it does not have gain and loss simultaneously in the longitudinal direction. As a result, the signal field intensity always decays because the corresponding imaginary part of susceptibilities is always positive. The field intensity propagation also gives agreement to the field susceptibilities shown in Fig. 3.

5. Conclusion

In this work, through the interaction with an ensemble of 4-level atoms in a double-Λ configuration, we reveal a scheme to simultaneously realize $\mathscr{P}\mathscr{T}$-symmetric and $\mathscr{P}\mathscr{T}$-antisymmetric conditions. It is the linearly increasing magnetic field that maps the spectrum information into

Optics EXPRESS

the longitudinal direction of wave propagation. Compared to previous proposals [8], in which different parameter conditions are needed for achieving $\mathscr{P}\mathscr{T}$-symmetry and $\mathscr{P}\mathscr{T}$-antisymmetry, our system provides a simple and all-optical-controllable way to realize $\mathscr{P}\mathscr{T}$-symmetry and $\mathscr{P}\mathscr{T}$-antisymmetry, as well as the switching process between them. With these phase-dependent susceptibilities, such a double-Λ system can provide a platform to study the field dynamics in $\mathscr{P}\mathscr{T}$-symmetry and $\mathscr{P}\mathscr{T}$-antisymmetry conditions.

Funding

Ministry of Science and Technology of Taiwan under Grant No. 105-2119-M-007-004.

References

1. C. M. Bender and S. Boettcher, "Real spectra in non-Hermitian Hamiltonians having $\mathscr{P}\mathscr{T}$-symmetry," Phys. Rev. Lett. **80**, 5243-5246 (1998).
2. Y.-C. Lee, M.-H. Hsieh, S. T. Flammia, and R.-K. Lee, "Local $\mathscr{P}\mathscr{T}$ symmetry violates the no-signaling principle," Phys. Rev. Lett. **112**, 130404 (2014).
3. S. Longhi, "Parity-time symmetry meets photonics: A new twist in non-Hermitian optics," Europhys. Lett. **120**, 64001 (2017).
4. C. E. Rüter, K. G. Makris, R. El-Ganainy, D. N. Christodoulides, M. Segev, and D. Kip, "Observation of parity-time symmetry in optics," Nature Phys. **6**, 192-195 (2010).
5. L. Chang, X. Jiang, S. Hua, C. Yang, J. Wen, L. Jiang, G. Li, G. Wang, and M. Xiao, "Parity-time symmetry and variable optical isolation in active-passive-coupled microresonators," Nat. Photonics **8**, 524-529 (2014).
6. Y.-C. Lee, J. Liu, Y.-L. Chuang, M.-H. Hsieh, and R.-K. Lee, "Passive PT-symmetric couplers without complex optical potentials," Phys. Rev. A **92**, 053815 (2015).
7. J.-H. Wu, M. Artoni, and G. C. La Rocca, "Parity-time-antisymmetric atomic lattices without gain," Phys. Rev. A **91**, 033811 (2015).
8. X. Wang and J.-H.. Wu, "Optical $\mathscr{P}\mathscr{T}$-symmetry and $\mathscr{P}\mathscr{T}$-antisymmetry in coherently driven atomic lattices," Opt. Express **24**, 4289-4298 (2016).
9. L. Praxmeyer, P. Yang, and R.-K. Lee, "Phase-space representation of a non-Hermitian system with $\mathscr{P}\mathscr{T}$ symmetry," Phys. Rev. A **93**, 042122 (2016).
10. R. El-Ganainy, K. G. Makris, D. N. Christodoulides, and Z. H. Musslimani, "Theory of coupled optical PT-symmetric structures," Opt. Lett. **32**, 2632-2634 (2007).
11. S. Klaiman, U. Gunther, and N. Moiseyev, "Visualization of branch points in $\mathscr{P}\mathscr{T}$-symmetric waveguides," Phys. Rev. Lett. **101**, 080402 (2008).
12. K. G. Makris, R. El-Ganainy, D. N. Christodoulides, and Z. H. Musslimani, "Beam dynamics in $\mathscr{P}\mathscr{T}$ symmetric optical lattices," Phys. Rev. Lett. **100**, 103904 (2008).
13. A. Guo, G. J. Salamo, D. Duchesne, R. Morandotti, M. Volatier-Ravat, V. Aimez, G. A. Siviloglou, and D. N. Christodoulides, "Observation of $\mathscr{P}\mathscr{T}$ symmetry breaking in complex optical potentials," Phys. Rev. Lett. **103**, 093902 (2009).
14. A. Regensburger, C. Bersch, M. A Miri, G. Onishchukov, D. N. Christodoulides, and U. Peschel, "Parity-time synthetic photonic lattices," Nature **488**, 167-171 (2012).
15. Z. H. Musslimani, K. G. Makris, R. El-Ganainy, and D. N. Christodoulides, "Optical solitons in $\mathscr{P}\mathscr{T}$ periodic potentials," Phys. Rev. Lett. **100**, 030402 (2008).
16. O. Bendix, R. Fleischmann, T. Kottos, and B. Shapiro, "Exponentially fragile $\mathscr{P}\mathscr{T}$ symmetry in lattices with localized eigenmodes," Phys. Rev. Lett. **103**, 030402 (2009).
17. C. Hang, Y. V. Kartashov, G. Huang, and V. V. Konotop, "Localization of light in a parity-time-symmetric quasi-periodic lattice," Opt. Lett. **40**, 2758-2761 (2015).
18. S. Longhi, "Bloch oscillations in complex crystals with $\mathscr{P}\mathscr{T}$ symmetry," Phys. Rev. Lett. **103**, 123601 (2009).
19. Y.-M. Liu, F. Gao, C.-H. Fan, and J.-H. Wu, "Asymmetric light diffraction of an atomic grating with PT symmetry," Opt. Lett. **42**, 4283-4286 (2017).
20. B. Peng, Ş. K. Ozdemir, F. Lei, F. Monifi, M. Gianfreda, G. L. Long, S. Fan, F. Nori, C. M. Bender, and L. Yang, "Parity-time-symmetric whispering-gallery microcavities," Nature Phys. **10**, 394-398 (2014).
21. M. G. Silveirinha, "Spontaneous parity-time-symmetry breaking in moving media," Phys. Rev. A **90**, 013842 (2014).
22. J. Schindler, A. Li, M. C. Zheng, F. M. Ellis, and T. Kottos, "Experimental study of active LRC circuits with $\mathscr{P}\mathscr{T}$ symmetries," Phys. Rev. A **84**, 040101(R) (2011).
23. W. Li, Y. Jiang, C. Li, and H. Song, "Parity-time-symmetry enhanced optomechanically-induced-transparency," Sci. Rep. **6**, 31095 p1-p11 (2016).
24. H. Kang, L. Wen, and Y. Zhu, "Normal or anomalous dispersion and gain in a resonant coherent medium," Phys. Rev. A **68**, 063806 (2003).
25. C. Hang, G. Huang, and V. V. Konotop, "$\mathscr{P}\mathscr{T}$ symmetry with a system of three-level atoms," Phys. Rev. Lett. **110**, 083604 (2013).

Optics EXPRESS

26. H.-J. Li, J.-P. Dou, and G. Huang, "PT symmetry via electromagnetically induced transparency," Opt. Express **21**, 32053-32062 (2013).
27. J. Sheng, M. A. Miri, D. N. Christodoulides, and M. Xiao, "$\mathscr{PT}$-symmetric optical potentials in a coherent atomic medium," Phys. Rev. A **88**, 041803 (2013).
28. Ziauddin, Y.-L. Chuang, and R.-K. Lee, "Giant Goos-Hanchen shift using $\mathscr{PT}$ symmetry," Phys. Rev. A **92**, 013815 (2015).
29. Ziauddin, Y.-L. Chaung, and R.-K. Lee, "$\mathscr{PT}$-symmetry in Rydberg atoms," Europhys. Lett. **115**, 14005 (2016).
30. Z.-Y. Liu, Y.-H. Chen, Y.-C. Chen, H.-Y. Lo, P.-J. Tsai, I. A. Yu, Y.-C. Chen, and Y.-F. Chen, "Large cross-phase modulations at the few-photon level," Phys. Rev. Lett. **117**, 203601 (2016).
31. N. I. Landy, S. Sajuyigbe, J. J. Mock, D. R. Smith, and W. J. Padilla,"Perfect metamaterial absorber," Phys. Rev. Lett. **100**, 207402 (2008).
32. Y.-D. Chong, L. Ge, H. Cao, and A. D. Stone, "Coherent perfect absorbers: Time-reversed lasers," Phys. Rev. Lett. **105**, 053901 (2010).
33. S. Longhi, "$\mathscr{PT}$-symmetric laser absorber," Phys. Rev. A **82**, 031801 (2010).
34. Y. Sun, W. Tan, H. Q. Li, J. Li, and H. Chen, "Experimental demonstration of a coherent perfect absorber with $\mathscr{PT}$ phase transition," Phys. Rev. Lett. **112**, 143903 (2014).
35. M. Kulishov, J. M. Laniel, N. Bélanger, J. Azaña, and D. V. Plant, "Nonreciprocal waveguide Bragg gratings," Opt. Express **13**, 3068–3078 (2005).
36. S. Longhi, "Invisibility in $\mathscr{PT}$-symmetric complex crystals," J. Phys. A **44**, 485302 (2011).
37. Z. Lin, H. Ramezani, T. Eichelkraut, T. Kottos, H. Cao, and D. N. Christodoulides, "Unidirectional invisibility induced by $\mathscr{PT}$-symmetric periodic structures," Phys. Rev. Lett. **106**, 213901 (2011).
38. L. Feng, Y.-L. Xu, W. S. Fegadolli, M.-H. Lu, J. E. B. Oliveira, V. R. Almeida, Y.-F. Chen, and A. Scherer, "Experimental demonstration of a unidirectional reflectionless parity-time metamaterial at optical frequencies," Nature Mater. **12**, 108–113 (2013).
39. J.-H. Wu, M. Artoni, and G. C. La Rocca, "Non-Hermitian degeneracies and unidirectional reflectionless atomic lattices," Phys. Rev. Lett. **113**, 123004 (2014).